D_2O). In the $2ROH/H_2O$ system, the k_1 value in eq 5 should be positive; i.e., $\alpha[NaCl] \leq 1$. Thus, the maximum value of $[NaCl]_{max}$ should be 5 M, whose value is close to the solubility of NaCl in H_2O. This observation suggests that the strong electrolyte of NaCl can be dissolved in water when water molecules are sufficient to hydrate both Na^+ and Cl^- ions, resulting in production of $(Na^+)_{hyd}$ and $(Cl^-)_{hyd}$. It is known that the hydration of inorganic ions including Na^+ and Cl^- is studied by means of the near-infrared method.[41] The hydrated ions $(Na^+)_{hyd}$ and $(Cl^-)_{hyd}$ are thermodynamically stable. Thus the addition of NaCl to water results in a decrease in the vapor pressure leading to the elevation of boiling point of the solution.

Concluding Remarks

The following conclusions can be drawn from the results of the excited-state proton-transfer reactions of naphthols with and without NaCl:

(1) The proton dissociation rate constant k_1 in the excited singlet state of naphthols decreases with an increase of [NaCl]. This decrease is caused by salt-induced destruction of water clusters, resulting in production the hydrated ions $(Na^+)_{hyd}$ and $(Cl^-)_{hyd}$. Water clusters, $(H_2O)_4$, act as acceptors for protons produced by deprotonation in the excited state of naphthols.

(2) The k_1 value in the presence of NaCl can be expressed as $k_1 = k_0[(H_2O)_4](1 - \alpha[NaCl])$, where $\alpha[NaCl] \leq 1$.

(3) The average hydration number of Na^+ or Cl^- is estimated as 4.4 or 6.6, respectively.

(4) The solubility (5.4 M) of NaCl in water is close to the maximum concentration of NaCl ($[NaCl]_{max} = 5$ M) calculated from the equation $\alpha[NaCl]_{max} = 1$ where $\alpha = 0.2$.

(5) The H–D kinetic isotope effect on k_1 in 2ROH* or 1ROH* is determined to be ca. 4.4 or 2.6, respectively, regardless of the concentration of NaCl.

Registry No. 1ROH, 90-15-3; 2ROH, 135-19-3; NaCl, 7647-14-5; H_2O, 7732-18-5; D_2, 7782-39-0; Na, 7440-23-5; Cl^-, 16887-00-6.

---

[41] Choppin, G. R.; Buijs, K. *J. Chem. Phys.* **1963**, *39*, 2042.

Experimental Determination of the OH Product Yield from NH_2 + NO at 300 K[†]

David A. Dolson

Environmental Science Department, General Motors Research Laboratories, Warren, Michigan 48090-9055

(Received: May 8, 1986; In Final Form: August 8, 1986)

The branching ratio, $\alpha = k_{1b}/k_{1a}$, has been experimentally determined at 300 K for two product channels of the NH_2 + NO reaction: $\rightarrow N_2 + H_2O$ (k_{1a}) and $\rightarrow N_2H + OH$ (k_{1b}). The reaction was studied in a fast-flow tube reactor coupled to a modulated-beam mass spectrometer. CO was added to scavenge hydroxyl radicals via $OH + CO \rightarrow CO_2 + H$. Separate experiments and kinetic modeling results confirm that the scavenging efficiency is near unity so that $[CO_2]$ is a good measure of [OH]. The branching ratio, $\alpha = [OH]/[H_2O] = [CO_2]/[H_2O]$, was determined from CO_2^+ and H_2O^+ ion intensities to be <0.15 at 300 K. This result is discussed as it relates to previous measurements and to the atmospheric chemistry of ammonia.

Introduction

The amidogen radical (NH_2) plays a pivotal role in the gas-phase atmospheric chemistry of ammonia. In the troposphere, NH_2 is primarily generated by the reaction of hydroxyl radicals with ammonia. Oxidation of ammonia, via reactions of O_3 and O_2 with NH_2, has been proposed as a natural source of atmospheric NO_x;[1] however, reactions of NH_2 with NO and NO_2 are known to be fast so that ammonia may also provide a natural atmospheric sink for NO_x. The rates and products of amidogen reactions with O_2, O_3, NO, and NO_2 determine whether ammonia behaves as a local source or sink for atmospheric NO_x.

A recent review[2] of amidogen reactivity indicates that some uncertainties in the kinetics and products of the NH_2 reactions remain to be solved. One of these concerns the yields of the several exothermic product channels of the reaction of NH_2 with NO. In particular, a current controversy centers on the relative yields of channels a and b of reaction 1.

$$NH_2 + NO \xrightarrow{k_{1a}} N_2 + H_2O \qquad (1a)$$

$$\xrightarrow{k_{1b}} N_2H + OH \qquad (1b)$$

The atmospheric implications of the NH_2 + NO reaction depend critically upon the relative yields of reactions 1a and 1b. If (1a) is dominant the result is that a reactive radical species is destroyed, yielding stable products and providing a sink for atmospheric NO. Conversely, if (1b) is dominant each NH_2 removed by NO generates one HO_2 (assuming that $N_2H \rightarrow N_2 + H$ is followed by $H + O_2 \rightarrow HO_2$ (M) or that $N_2H + O_2 \rightarrow N_2 + HO_2$ occurs) and one OH radical. In this second case NO is still removed, but two reactive radicals are generated for each NH_2 lost.

Historically, experimental results from the photolysis of NH_3 + NO mixtures have indicated that the quantum yield for N_2 production, ϕ_{N_2}, is near unity for reaction 1 at ~300 K.[3-6] Gehring et al.[7] observed N_2 and vibrationally excited water as products in a discharge flow study of reaction 1. These results would seem to present an overwhelming argument for the primary importance of (1a). However, several authors,[8-12] in modeling the $NH_3/NO/O_2$ reaction system at 1000–1500 K, have found it essential to include a significant yield for the chain-branching

---

[†] Presented at the 190th National Meeting of the American Chemical Society, Chicago, IL, September 8–13, 1985.

(1) McConnell, J. C. *J. Geophys. Res.* **1973**, *78*, 7812.
(2) Lesclaux, R. *Rev. Chem. Intermed.* **1984**, *5*, 347.
(3) Bamford, C. H. *Trans. Faraday Soc.* **1939**, *35*, 568.
(4) Serewicz, A.; Noyes, W. A., Jr. *J. Phys. Chem.* **1959**, *63*, 843.
(5) Srinivasan, R. *J. Phys. Chem.* **1960**, *64*, 679.
(6) Jayanty, R. K. M.; Simonaitis, R.; Heicklen, J. *J. Phys. Chem.* **1976**, *80*, 433.
(7) Gehring, M.; Hoyermann, K.; Schacke, H.; Wolfrum, J. *Symp. (Int.) Combust., [Proc.] 14th* **1973**, 99.
(8) Miller, J. A.; Branch, M. C.; Kee, R. J. *Combust. Flame* **1981**, *43*, 81.
(9) Salimian, S.; Hanson, R. K. *Combust. Sci. Technol.* **1980**, *23*, 225.
(10) Dean, A. M.; Hardy, J. E.; Lyon, R. K. *Symp. (Int.) Combust., [Proc.] 19th* **1982**, 97.
(11) Silver, J. A. "A Chemical Model for the Reduction of Nitric Oxide by Ammonia in Post Combustion Flows"; Aerodyne Research, Inc., Report No. RR-281, 1981.
(12) Dasch, C. J.; Blint, R. J. *Combust. Sci. Technol.* **1984**, *41*, 223.

0022-3654/86/2090-6714$01.50/0

product channel (1b). Miller et al.[8] have proposed (1b) as the dominant channel for $T < 1500$ K. They argued that (1b) followed by secondary reactions yielding $N_2 + H_2O$ as final products would be consistent with the observations of Gehring et al.[7] Subsequently, three direct experimental measurements of the OH product yield at ~300 K were accomplished with laser-excited fluorescence[13,14] and resonance fluorescence[13,15] detection of OH. Silver and Kolb[13] found the OH yield to be about 40% of the total NH_2 reacted in a discharge flow study while Andresen et al.[14] have reported ≥65% OH yield in a 193-nm laser photolysis experiment. Stief et al.[15] detected no OH product in a flash photolysis study of reaction 1 and reported <22% as a conservative upper limit. Thus the experimental results support two conflicting views concerning the absolute yield of the chain-branching channel, and the reasons for this discrepancy are not clear.

The present study was undertaken to determine the branching ratio, $\alpha = k_{1b}/k_{1a}$, at 300 K. Consequently, it focuses on both product channels in contrast to the recent absolute OH yield experiments[13-15] that concentrate primarily upon (1b). The α used here to denote the k_{1b}/k_{1a} branching ratio should not be confused with the same symbol used by others[13] to denote the absolute OH yield. The discharge flow technique used here includes efficient scavenging of OH and product detection by modulated-beam mass spectrometry. Hydroxyl scavenging by CO suppresses the secondary reactions proposed by Miller et al.[8] which might otherwise lead to an erroneous interpretation of the results.

Experimental Design and Apparatus

Amidogen radicals are generated efficiently in a flow tube from the reaction of F atoms with ammonia.

$$F + NH_3 \rightarrow HF + NH_2 \qquad (2)$$

Recent measurements[16,17] suggest $0.3 \times 10^{-10} < k_2 \leq 1.0 \times 10^{-10}$ cm^3 molecule^{-1} s^{-1}, and several investigators[2] have found the reaction to be a reasonably "clean" source of NH_2. NO and CO are added downstream from the ammonia injection point, and the reactions

$$NH_2 + NO \rightarrow N_2 + H_2O \qquad (1a)$$

$$\rightarrow N_2H + OH \qquad (1b)$$

$$OH + CO \rightarrow H + CO_2 \qquad (3)$$

are given sufficient time for completion before sampling of the gas mixture occurs. Scavenging the hydroxyl radicals with CO yields a twofold advantage in this study. First, the fact that k_3[CO] can be made quite fast by choosing a high CO concentration enables the suppression of competing OH loss channels such as wall losses and reactions with other radical species and with NH_3. Second, it can be shown that the branching ratio can be expressed as

$$\alpha = \frac{k_{1b}}{k_{1a}} = \frac{[CO_2]}{[H_2O]} \qquad (4)$$

for time $t > (5k_3[CO])^{-1}$ when (3) is the only important loss process for OH. Thus the branching yield is obtained from measurements of the CO_2^+ and H_2O^+ ion signals at m/e 44 and 18, respectively, in a modulated-beam mass spectrometer. While a quantitative determination of [OH] from the m/e 17 ion signal would be very difficult in the presence of NH_3, no interference in the CO_2 measurement at m/e 44 is expected since there is general agreement[2] that the absolute N_2O yield from (1) is <0.01. It is also noteworthy that the relative detection efficiencies for CO_2 and H_2O can be easily determined from gas mixtures of known composition. This is in contrast to the experimental determinations of the absolute OH yield from (1)[13-15] where it is more difficult to accurately determine the detection efficiencies for reactive radical species such as NH_2 and OH.

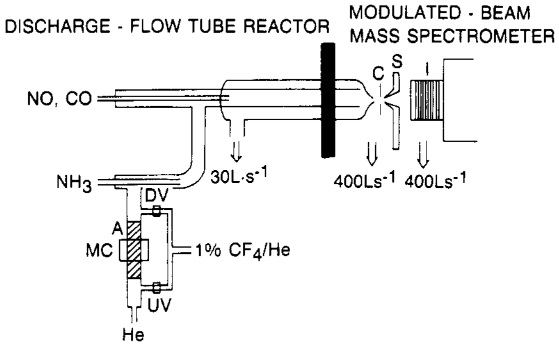

Figure 1. Schematic diagram (not to scale) of the flow reactor and mass spectrometer apparatus. UV and DV are computer-controlled solenoid valves for the addition of CF_4/He upstream and downstream of the electrodeless discharge plasma. A, $^1/_2$-in.-o.d. alumina tube. MC, microwave cavity. C, 400-Hz tuning fork chopper. S, 0.2-cm-diameter skimmer cone. I, axial beam ionizer. The distance from the ~0.05-cm-diameter sampling orifice in the flow tube to the skimmer is approximately 1 cm.

The discharge-flow tube reactor and the modulated-beam mass spectrometer are schematically detailed in Figure 1. The 0.95-cm-i.d. glass flow tube is 34 cm in length and has a side arm in which NH_2 is generated from the reaction of F atoms with ammonia. F atoms are obtained by passing 1% CF_4/He through a 2450-MHz microwave discharge plasma contained in a 1.25-cm-o.d. alumina tube. The plasma is maintained in the main flow of helium with 10–14 W of power in an Evenson cavity.[18] The CF_4 mixture is added to the helium flow either upstream (F atoms on) or downstream (F atoms off) from the plasma by means of two solenoid valves.

Stainless steel or Pyrex injectors are used to add NH_3 in the side arm and NO and CO together in the main part of the flow reactor. All surfaces exposed to the gas flow are coated with a halocarbon wax[19] to minimize wall-catalyzed reactions. Although several alternative injector positions and reactant addition schemes were evaluated in preliminary experiments, the results to be presented here were obtained with a spacing of 22 cm from the microwave cavity to the NH_3 injector, 12 cm between injectors, and 24 cm from the NO and CO injector to the sampling point. Under typical flow conditions of 16.7 m·s^{-1}, the reaction time between injectors is 7 ms, and 14 ms is available between the addition of NO and CO and the sampling of the reactor gases. The total pressure is measured with a capacitance manometer[20] at the exit of the flow tube. All gas flow rates are controlled by calibrated mass flow controllers,[21] and copper or Teflon tubing is used throughout. Gases are exhausted through a throttled mechanical pump[22] rated at 30 L·s^{-1}.

A fused silica discharge tube was used in preliminary experiments. Large signals at m/e 28 (CO^+, Si^+), 32 (O_2^+), 44 (CO_2^+, SiO^+), and 47 (FCO^+, SiF^+) were observed upon passing CF_4 through the discharge plasma in helium. Higher masses were not searched. Substitution of the alumina tube reduced the F atom signal by 50%, but the signals mentioned above were reduced by more than an order of magnitude. This behavior is in agreement with the CF_4 discharge observations of Kolb and Kaufman.[23] A small m/e 44 signal remained even with the alumina tube. The measured CO_2^+ intensities always contained this contribution.

The flow tube enters the differentially pumped mass spectrometer[24] through an o-ring-sealed vacuum coupling. Gases

---

(13) Silver, J. A.; Kolb, C. E. *J. Phys. Chem.* **1982**, *86*, 3240.

(14) Andresen, P.; Jacobs, A.; Kleinermanns, C.; Wolfrum, J. *Symp. (Int.) Combust.*, *[Proc.]* *19th* **1982**, 11.

(15) Stief, L. J.; Brobst, W. D.; Nava, D. F.; Borkowski, R. P.; Micheal, J. V. *J. Chem. Soc., Faraday Trans. 2* **1982**, *78*, 1391.

(16) Walther, C.-D.; Wagner, H. Gg. *Ber. Bunsen-ges Phys. Chem.* **1983**, *87*, 403.

(17) Manocha, A. S.; Setser, D. W.; Wickramaaratchi, M. A. *Chem. Phys.* **1983**, *76*, 129.

(18) Opthos Instruments, Rockville, MD.

(19) Halocarbon Products Corp., Hackensack, NJ; Series 15-00.

(20) MKS Instruments Inc., Burlington, MA; Model 222 BHS-10 torr.

(21) Tylan Corp., Carson, CA; Model FC-260.

(22) Leybold-Heraeus, San Jose, CA; Model DK-100.

(23) Kolb, C. E.; Kaufman, M. *J. Phys. Chem.* **1972**, *76*, 947.

(24) Extranuclear Laboratories, Pittsburgh, PA; EMBA-II with 041-1 ionizer, 270-9 mass filter, and 032-3 counting preamp.

TABLE I: Signal Averager Input Selection

input	F atoms	molecular beam chopper
1	on	open
2	on	closed
3	off	open
4	off	closed

exiting the flow tube through the 0.05-cm-diameter orifice form a molecular beam that is chopped at 400 Hz and skimmed with a 0.20-cm-diameter cone. A portion of the beam is ionized in an axial beam ionizer, mass analyzed, and detected with a channel electron multiplier.[25] The multiplier signal is fed to one of two preamplifier–discriminator circuits,[24,26] and the resulting TTL pulses are directed by a homemade digital switching circuit to the appropriate multichannel scaling inputs of a dedicated signal-averaging computer.[27] The ionizer was operated at 40 eV with an electron current of 1.5 mA. Ion signals were observed to vary linearly with concentration under these conditions.

A microcomputer CAMAC system[28] is used to scan the mass ranges of interest and to operate the solenoid valves that control the F atom generation. Data acquisition by the signal averager is synchronized to the solenoid operation and mass selection through the switching circuit by an empirically determined programmed delay of of the mass-scanning algorithm. In a typical experiment an initial mass scan is accomplished with the CF_4 added upstream of the discharge plasma, and the detected ion pulses are directed by the switching circuit to inputs 1 and 2 of the signal averager. At the end of this scan the CF_4 addition is switched to the downstream point, and a 3.8-s delay is imposed for gas-flow stabilization before triggering the next mass sweep. Inputs 3 and 4 are used as the same mass ranges are rescanned without F atom generation. This process is repeated for several pairs of mass scans, with a 3.8-s delay each time the CF_4 addition point is changed, until the signal-to-noise ratio is sufficiently high. At the end of such an experiment, the quadrant of memory allocated to each of the four data inputs contains a mass spectrum for the conditions of Table I. This procedure is an extension of the standard phase-sensitive ion-counting method.[29,30] The mass spectrum of the reactor gases in the molecular beam without F atom generation is obtained by a point by point subtraction of quadrant 4 (background alone) from quadrant 3 (molecular beam + background). Similary the "F atoms on" molecular beam mass spectrum is given by subtracting quadrant 2 from quadrant 1. The desired information in this study is the $[CO_2]/[H_2O]$ ratio and is obtained from the difference of these two spectra, $(1 - 2) - (3 - 4)$, in order to correct for small amounts of these species present as impurities. Up to 10 masses of interest in four separate regions are observed, depending upon the experiment, and the regions are completely scanned as opposed to monitoring only peak intensities. Integrated peak intensities are obtained by summing the digital values in the several channels defining an ion peak. With typical scan durations of ~60 s for a maximum of 350 total scans, up to 6 h are required for data acquisition. The low-frequency (~0.02-Hz) modulation of F atoms eliminates the long-term drift problems that might be encountered if a long acquisition time were to be devoted to the "F atoms on" mass scans followed by the same time period of "F atoms off" scans. It should be noted that while an up–down counting technique[29] might be used to provide the chopper open minus chopper closed spectrum equivalent to $(1 - 2)$ or $(3 - 4)$, the statistical uncertainties in the resultant mass spectrum can only be determined if the background intensities are known.[30]

Ammonia (99.99%), 1% CF_4 (99.0%) in helium (99.9999%), CO (99.5%), and helium (99.9999%) were used without further purification except for passing the CF_4/He and He through 77K traps between the flow controllers and the reactor. Nitric oxide (99.0%) was passed through silica gel at 195 K immediately upstream of the flow controller in order to remove NO_2 and N_2O impurities. Ar (99.999%), 2% in helium (99.9999%), was used at times as an inert tracer to monitor detection stability, and research grade CO (99.99%) was used in some experiments. The same results were obtained with either CO sample. Calibration mixtures of CO_2 (99.8%) and deionized water in helium were prepared in 1- or 2-L Pyrex sample bulbs after degassing the water thoroughly. Pressures were measured with a 0–10-Torr capacitance manometer or a 0–800-Torr bourdon gauge.

TABLE II: Experimental Conditions[a]

	side arm	flow tube
$[NH_3]$	1.3 (14)[b]	1.0 (14)
$[NH_2]$	1.3 (13)[c]	0.1–0.2 (13)[d]
$[NO]$		2.4 (14)
$[CF_4]$	5.8 (13)[b]	4.9 (13)[b]
$[CO]$		5.2 (15)
$[He]$	3.2 (16)	2.7 (16)
linear flow velocity	13.9 m s^{-1}	16.6 m s^{-1}
$k_2[NH_3]$	9100 s^{-1}	
$k_1[NO]$		4100 s^{-1}
$k_3[CO]$		780 s^{-1}
$k_{OH+NH_3}[NH_3]$		16 s^{-1}

[a] Concentrations in molecule cm^{-3} are calculated near the injection points assuming plug flow conditions, 1.3 (14) = 1.3×10^{14}. Flow tube values for some species reflect the dilution due to the addition of CO and NO. The pressure drop correction would raise these values by no more than ~25%. Conditions are "F atoms on" unless otherwise noted. [b] F atoms off. [c] This is the value of [F] determined by titration with H_2 or with NH_3. [d] An approximate 10-fold reduction of $[NH_2]$ occurs in the side arm due to wall losses and to $NH_2 + NH_2 \rightarrow$ products.

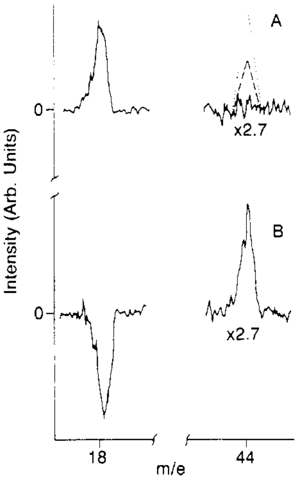

Figure 2. *m/e* 18 (H_2O^+) and 44 (CO_2^+) regions of the difference mass spectra obtained in two separate experiments described in the text. Intensities in the CO_2^+ region have been scaled by a factor of 2.7 so that the figure displays H_2O^+ and CO_2^+ signals with equal sensitivity. The (A) spectrum is from the NH_2 + NO reaction in the presence of CO. See Table II for details. The H_2O^+ signal confirms H_2O as a primary product since OH is scavenged by CO and cannot undergo secondary reactions to produce H_2O. The very small CO_2^+ signal is revealed only by integrating the peak intensity. The branching ratio obtained from this spectrum is $\alpha = [CO_2]/[H_2O] = 0.07$ ($\sigma = 0.04$). The results of ref 13 (dashed line) and 14 (dotted line) are indicated as idealized triangular peaks for comparison with this experiment. See the text for details. The (B) spectrum is from an experimental test of the scavenging efficiency. Hydroxyl radicals are generated via $F + H_2O \rightarrow HF + OH$ in the presence of CO. The negative signal at *m/e* 18 is due to the H_2O lost with F atoms on. The CO_2^+ and H_2O^+ integrated intensities are identical, and for this experiment the scavenging efficiency $\epsilon_3 = 1.00$ ($\sigma = 0.14$).

Results and Discussion

The k_{1b}/k_{1a} branching ratio was determined at 300 K from the $[CO_2]/[H_2O]$ product ratio in the reaction mixture sampled after

---

(25) Gallileo Electro-Optics Corp., Sturbridge, MA; Model 4830.
(26) Amptek, Bedford, MA; Model A-101.
(27) Tracor Northern, Middleton, WI; TN1710, -42, -48.
(28) Kinetic Systems, Lockport, IL; Model 8010.
(29) Calo, J. M.; Bailey, A. D. *Rev. Sci. Instrum.* **1974**, *45*, 1325.
(30) Foner, S. N. *Adv. At. Mol. Phys.* **1966**, *2*, 385.

sufficient time for completion of the hydroxyl scavenging reaction. Experimental conditions are listed in Table II, where the concentrations are calculated from the calibrated flow rates by assuming plug flow conditions. The m/e 18 and 44 regions of a difference spectrum obtained under these conditions are displayed in Figure 2a. The scaling factor used for the m/e 44 region was determined by introducing known mixtures of CO_2 and H_2O in helium into the gas flow. Using these calibrant mixtures alone gave the same results. The relative detection sensitivity is given by

$$\frac{[CO_2]}{[H_2O]} = (2.7 \pm 0.3)\frac{I_{44}}{I_{18}} \qquad (5)$$

where I_M is the integrated peak intensity for mass M. With (5), the branching ratio obtained from the difference spectrum in Figure 2a is $\alpha = 0.07 \pm 0.04$, where the uncertainty is one standard deviation from particle counting statistics. The experiment was repeated 3 more times and yielded $\alpha = 0.11$, 0.01, and 0.08. The scatter in these values reflects the precision of obtaining the very small CO_2^+ difference signal, which is typically only <3% of the m/e 44 background signal (input 4 of Table I). An average value, weighted according to the number of scans for each result, was calculated to be $\alpha = 0.05$. With an allowance for statistical and estimated uncertainties, a resonable upper limit at 300 K is $\alpha < 0.15$.

This branching ratio measurement is uncorrected for three anomalous contributions to the CO_2^+ ion signal. The first contribution arises from a small amount of CO_2 produced in the CF_4 discharge. The second source is due to the residual H_2O in the CF_4/He mixture. Hydroxyl is generated by passing H_2O through the discharge and/or by reaction 6 between the discharge tube and the NH_3 injection point. Some of the OH will react with NH_3 and NH_2 in the side arm to reproduce the initial H_2O, and the remaining OH will produce CO_2 in reaction 3. The net result in the difference spectrum is increased $[CO_2]$ and decreased $[H_2O]$. A third anomalous contribution to the m/e 44 difference signal may result from the generation of NH in the side arm by $F + NH_2 \rightarrow HF + NH$.[16] Exothermic product channels for the reaction of NH with NO include $N_2O + H$ and $N_2 + OH$. Each of these channels produces a m/e 44 product, either directly or via reaction 3. Experiments in which NO and CO were separately omitted indicate that while these anomalous m/e 44 sources are small on an absolute scale together they constitute a significant portion of the m/e 44 signal attributed to reaction 1b. Consequently, the true k_{1b}/k_{1a} ratio is probably lower than the measured values.

Separate experiments, without NH_3 or NO, were carried out in order to test the scavenging efficiency of (3). In these experiments 2% Ar/He was passed through water in a two-stage bubbler maintained at a constant temperature within ±2 K. This gas flow was added to the reactor with CO through the main injector, and the reaction

$$F + H_2O \rightarrow HF + OH \qquad (6)$$

generated OH in the presence of CO just as (1b) might do. The scavenging efficiency, ϵ_3, is determined from the ratio of $[CO_2]$ produced in (3) to $[H_2O]$ lost in (6). The m/e 18 and 44 regions of a difference spectrum obtained in this test appear in Figure 2b. The results of three experiments yielded a weighted average, $\epsilon_3 = 0.96 \pm 0.17$, where the uncertainty is 1σ. In these experiments [CO] was kept within 10% of 5×10^{15} molecule cm^{-3}, [F] $\sim 1.3 \times 10^{13}$ molecule cm^{-3}, and $[H_2O]/[F]$ ranged from 2.3 to 22. That ϵ_3 was high even with the lowest $[H_2O]/[F]$ ratio suggests that CO competed favorably for OH against wall losses *and* against radical–radical reactions such as

$$F + OH \rightarrow HF + O \qquad (7)$$

and

$$OH + OH \rightarrow H_2O + O \qquad (8)$$

Thus the scavenging technique works well for the conditions of this test.

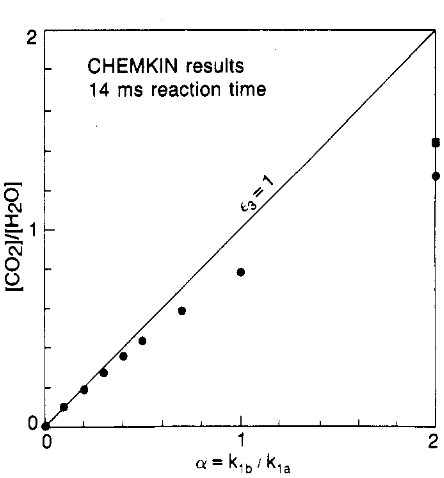

Figure 3. CHEMKIN modeling results of the OH + CO scavenging efficiency in the NH_2 + NO reaction system. The solid line represents unit scavenging efficiency, $[CO_2] = [OH]$, for which the $[CO_2]/[H_2O]$ ratio is a good measure of k_{1b}/k_{1a}. The solid circles are the model predictions for the flow tube concentrations of Table II. The initial $[NH_2]$ is 2×10^{12} molecule cm^{-3}, and a 14-ms reaction time is used to simulate the injector–sampling orifice flow time. The solid square at $\alpha = 2$ is from the same calculation with $[NH_2] = 1.2 \times 10^{12}$ molecule cm^{-3}.

Other secondary reactions are possible in the study of NH_2 + NO, and it was suggested that modeling the reactions in this system would be instructive in evaluating the scavenging efficiency as a function of the branching ratio.[31] The qualitative expectation is that as the branching ratio increases the scavenging efficiency decreases due to increasing competition for hydroxyl by N_2H and HNO. A model of 19 species and 32 reactions, including many from ref 8, 12, and 32, was evaluated with the CHEMKIN[33] code. Reactions requiring high activation energies or third bodies were excluded from this modeling effort due to the experimental constraints of 1-Torr total pressure at 300 K. Reactions involving CO and HCO were also included, but HCO was found to be relatively unimportant since $HCO + NO \rightarrow HNO + CO$ is fast.[34,35] The initial conditions supplied to the model are the flow tube concentrations of Table II, with the exclusion of CF_4. The calculated concentrations at 14 ms were used to evaluate the scavenging efficiency, and the results are displayed in Figure 3. The calculated ratio, $[CO_2]/[H_2O]$, is plotted against the k_{1b}/k_{1a} branching ratio that is used in the model ($k_{1a} + k_{1b} = 1.7 \times 10^{-11}$ cm^3 molecule^{-1} s^{-1}). The qualitative expectations are verified in this figure. As k_{1b}/k_{1a} increases, the $[CO_2]/[H_2O]$ ratio falls away from the solid line that indicates unit scavenging efficiency. It is important to note that $[CO_2]/[H_2O]$ is a very good measure of the branching ratio for $\alpha \leq 0.4$ with no more than ~10% error. Rate constants for OH reactions that produce H_2O were increased to 1.7×10^{-10} cm^3 molecule^{-1} s^{-1} in a more severe test of the modeled scavenging efficiency. At $\alpha = 2.0$ the calculated scavenging efficiency decreased from 65% to 40%, but it remained above 85% for $\alpha \leq 0.2$. Consequently the experimental result, $\alpha = [CO_2]/[H_2O] < 0.15$, determined by the scavenging technique is supported by both a separate experimental check and by modeling evidence as a convincing upper limit of k_{1b}/k_{1a} at 300 K.

This result agrees well with several previous investigations[3-7] including the direct experiment of Stief et al.,[15] whose $k_{1b}/k_1 < 0.22$ result corresponds to $\alpha < 0.25$. It is also in good agreement with the *tentative* result of Dreier et al.,[36] who used this same

---

(31) This suggestion was made by R. J. Blint and by J. A. Miller.

(32) Baulch, D. L.; Cox, R. A.; Crutzen, P. J.; Hampson, R. F., Jr.; Kerr, J. A.; Troe, J.; Watson, R. T. *J. Phys. Chem. Ref. Data* **1982**, *11*, 327.

(33) Kee, R. J.; Miller, J. A.; Jefferson, T. H. SAND 80-8003, Sandia National Laboratories, 1980.

(34) Clark, J. H.; Moore, C. B.; Nogar, N. S. *J. Chem. Phys.* **1978**, *68*, 1264.

(35) Veyret, B.; Lesclaux, R. *J. Phys. Chem.* **1981**, *85*, 1918.

(36) Dreier, T.; Jacobs, A.; Schneider, M.; Wolfrum, J. Presented at the 182nd National Meeting of the American Chemical Society, New York, NY, August, 1981; paper PHYS 4.

hydroxyl scavenging reaction with resonance absorption detection of hydrogen atoms. No increase in [H] due to (3) was observed in the experiment, and the absolute OH yield in (1) was found to be less than 15% ($\alpha < 0.13$). This experiment apparently has been discounted by Andresen et al.[14] although they state that "The reason why ... OH + CO → CO_2 + H did not show the expected increase in H-atom concentration is not clear."

The results of Silver and Kolb[13] and of Andresen et al.[14] correspond to $\alpha = 0.7$ and $\alpha \geq 1.8$, respectively. They are indicated as idealized triangular peaks in Figure 2a for comparison with this experiment. The peak heights are not α directly but rather the model predictions of Figure 3: $[CO_2]/[H_2O] = 0.6$ and 1.2 for $\alpha = 0.7$ and 1.8, respectively. Thus the peaks represent expected signals corresponding to agreement with the results of ref 13 and 14. Signals of these magnitudes would have been easily detected in this experiment. Reasons for the obvious disagreement between this work and two[13,14] of the three direct observations are not known; however, the evidence is now strongly weighted against a significant OH yield at 300 K. The scavenging technique suppresses secondary reactions involving OH so that the water observed in Figure 2a is a primary product of (1a). Since the tested reaction 3 did not produce significant amounts of CO_2, the inescapable conclusion is that the OH yield is small. Furthermore, as observed by Michael,[37] a high yield of OH is not compatible with the static photolysis results using excess NH_3. The subsequent chain reaction involving $OH + NH_3 \rightarrow NH_2 + H_2O$ would undoubtedly lead to a higher yield of N_2 than the observed $\phi_{N_2} = 1$. Yet another argument against the importance of (1b) at 300 K is provided by the ab initio calculations concerning the stability of N_2H.[38] The results indicate that at 300 K it is not likely that N_2H should survive for more than 2×10^{-9} s. When tunneling is included, the lifetime of N_2H is reduced to $\sim 5 \times 10^{-11}$ s. Thus N_2H should unimolecularly dissociate to N_2 + H, and that H atoms are not observed[7,13,14,39] from (1) is strong evidence against (1b). In the experiment of Gehring et al.[7] N_2H would not have survived long enough to react with OH or NO as proposed by Miller et al.[8]

Some *speculation* may be offered concerning the direct observation of OH by Andresen et al.[14] Their Figure 4 indicates that [H] after the 90-mJ 193-nm laser pulse is 5 times greater than expected from the NH_3 absorption cross section,[40] assuming a 3 cm^2 excimer beam area. Whyte and Phillips[39] interpreted a similar observation as the result of multiphoton dissociation (MPD) of NH_3 to a mixture of NH_2, NH, N, and H. They avoided MPD only with pulse energies of <5 mJ and found that complete dissociation to atoms occurred with ≥20-mJ pulse energies. Andresen et al.[14] used the H atoms from the ammonia photolysis pulse to generate hydroxyl via $H + NO_2 \rightarrow NO + OH$ in order to calibrate the absolute OH yield in (1). Implicit in this procedure is the assumption that the only photolysis process is $NH_3 \rightarrow NH_2 + H$ so that $[H] = [NH_2]$. If MPD played a significant role in these experiments, the calibration technique would tend to underestimate k_{1b}/k_1 since $[H] > [NH_2]$. A consequence of this effect is that for $[H] > 1.5[NH_2]$ the reported 65% OH yield, when corrected, exceeds the allowable 100% maximum value. Since $[H] \gg [NH_2]$ has now been demonstrated for 193-nm pulse energies of ≥20 mJ,[39] it would seem reasonable that there is an alternate explanation for their observation of OH. Perhaps the most plausible source of OH is the dissociation of the vibrationally excited H_2O^* product of (1a) by the high-energy probe laser pulses. This possible explanation of the OH source is also consistent with the reported common appearance rates of H_2O^* and OH. The speculations offered in this paragraph could be tested by varying the laser fluences.

Concluding Remarks

Experimental evidence at 300 K argues strongly for a small branching ratio, $k_{1b}/k_{1a} < 0.15$, although two previous direct measurements disagree. The present results say nothing about the 1000 K < T < 1500 K temperature region, for which the chain branching channel was initially postulated.[8] The possibility of a temperature-dependent branching ratio has not been tested.

The atmospheric significance of the small branching ratio is that reaction 1 is almost exclusively a chain termination reaction that yields unreactive products. Whether atmospheric ammonia is a source or a sink of NO_x is determined by the local concentrations of O_3, NO, and NO_2. With the rate coefficients from Lesclaux,[2] atmospheric reactions of NH_2 favor NO_x production only when $[O_3]/([NO] + [NO_2]) \gtrsim 120$. This condition is most commonly found in rural areas where $[NO_x]$ is low. The partitioning of NH_3 loss between gas-phase photochemistry, aerosol formation, and rainout mechanisms must be more fully studied in order to evaluate the sensitivity of NO_x levels to atmospheric ammonia.

Note Added in Proof. Two experiments concerning the OH yield of this important reaction were published after this article was submitted. Hall et al.[41] reported a 13 ± 2% OH yield at room temperature. Their result agrees with the upper limit reported here and with the work of Stief et al.[15] Kimball-Linne and Hanson[42] reported OH yields of 48% and ≥80% at 1050 and 1400 K, respectively.

Acknowledgment. Several discussions with the following people have provided insight and encouragement during this investigation; Dick Blint, Alan Dunker, Joe Michael, Joel Silver, and Tom Sloane. Dick Blint and Alan Dunker have been particularly helpful in providing the CHEMKIN package and instructions for its use. I thank John Ratcliffe and Robert Stephens for assistance with the experimental apparatus.

Registry No. NH_2, 13770-40-6; NO, 10102-43-9.

---

(37) Michael, J. V. in the discussion of ref 10.

(38) Curtiss, L. A.; Drapcho, D. L.; Pople, J. A. *Chem. Phys. Lett.* **1984**, *103*, 437.

(39) Whyte, A. R.; Phillips, L. F. *J. Phys. Chem.* **1984**, *88*, 5670.

(40) Suto, M.; Lee, L. C. *J. Chem. Phys.* **1983**, *78*, 4515.

(41) Hall, J. L.; Zeitz, D.; Stephens, J. W.; Kasper, J. V. V.; Glass, G. P.; Curl, R. F.; Tittel, F. K. *J. Phys. Chem.* **1986**, *90*, 2501.

(42) Kimball-Linne, M. A.; Hanson, R. K. *Combust. Flame* **1986**, *64*, 337.